A HYBRID CONVOLUTIONAL NEURAL NETWORK-EXTREME LEARNING MACHINE WITH AUGMENTED DATASET FOR DNA DAMAGE CLASSIFICATION USING COMET ASSAY FROM BUCCAL MUCOSA SAMPLE

Yues Tadrik Hafiyan[1], Afiahayati[1,*], Ryna Dwi Yanuaryska[2]
Edgar Anarossi[3], Vincent Michael Sutanto[1], Joko Triyanto[1]
and Yasubumi Sakakibara[4]

[1]Department of Computer Science and Electronics
Faculty of Mathematics and Natural Sciences
Universitas Gadjah Mada
Sekip Utara, Bulaksumur, Sleman, Special Region of Yogyakarta 55281, Indonesia
*Corresponding author: afia@ugm.ac.id

[2]Department of Radiology Dentomaxillofacial
Faculty of Dentistry
Universitas Gadjah Mada
Jl. Denta 1, Sekip Utara, Yogyakarta 55281, Indonesia

[3]Robot Learning Laboratory
Division of Information Science
Nara Institute of Science and Technology
8916-5 Takayama-cho, Ikoma, Nara 630-0192, Japan

[4]Department of Biosciences and Informatics
Faculty of Science and Technology
Keio University
3-14-1 Hiyoshi, Kohoku-ku, Yokohama, Kanagawa 223-8522, Japan

ABSTRACT. *DNA is the information carrier in cells that are susceptible to damage, either naturally or due to external influences. Comet assays are often used by experts to determine the level of damage. However, the comet assays gathered with swab technique (Buccal Mucosa for example) often produced a higher noise level compared to ones that are cell-cultured, thus, making the analysis process more difficult. In this research, we proposed a novel way to assess the degree of damage from Buccal Mucosa comet assays using a hybrid of Convolutional Neural Network (CNN) and Extreme Learning Machine (ELM). The CNN was used to capture and extract spatial relation from every comet, while the ELM was used as a classifier that can minimize the risk of vanishing gradient. Our hybrid CNN-ELM model scored 96.96% for accuracy, while the VGG16-ELM scored 88.4% and ResNet50-ELM 76.8%.*
Keywords: Buccal Mucosa, Comet assay, Convolutional neural network, Extreme learning machine

1. **Introduction.** DNA is one of the important components in the human body that carries information that is passed on to the cells of its offspring [1]. As the smallest component in cells, DNA does not escape from the possibility of being damaged. Comet assay or Single-Cell Gel Electrophoresis (SCGE) is often used in assessing the degree of DNA damage [1]. According to [2], DNA damage can also be caused by exposure to

ionic radiation during the radiography process, even at low doses. The Buccal Mucosa is directly exposed to the cytotoxic/genotoxic agent affecting the oral cavity and hence can be used as a suitable sample for analyzing DNA damage. Moreover, the Buccal Mucosa cells swab is the preferred harvesting procedure as it is less invasive than lymphocytes cell culture and does not cause discomfort to the patients [2]. However, the swabbing procedure has its drawback, as the swab activity may produce higher noise, thus, making the analysis process more difficult.

The degree of DNA damage is often assessed by experts, but computational methods are often used as an alternative. Several software was developed to measure the degree of DNA damage, which is COMET Assay IIITM [3], Komet version 5.5 [4], and Comet Assay Software Project (CASP) 1.2.2 [5,6] and a free software, OpenComet [7]. They were designed for the sample from lymphocytes cell culture. They perform well on comet assay from lymphocytes cell culture, but not from Buccal Mucosa swab. Because of the low accuracy score, a specific computational method is required to detect the degree of damage from the Buccal Mucosa swab.

[8] proposed a transfer learning approach to assess the degree of damage specifically for Buccal Mucosa comet assays. The research used VGG16 as the feature extractor, while multi-layered perceptron was used as its classifier. The dataset used was considered tiny and was classified using a deep architecture, thus, resulting in the model producing 70.5%. The deep architecture used by this research was also prone to vanishing gradient problem that often occurred in backpropagation process [6]. The accuracy score was relatively low; therefore, a better computational method must be proposed to resolve this problem. [9] used extreme learning machines and showed that this method can produce a high level of accuracy and very fast computation time. The simplicity of extreme learning machine architecture makes this architecture not vulnerable to vanishing gradients as experienced in [8].

[10-12] proposed a hybrid architecture of Convolutional Neural Network (CNN) and Extreme Learning Machine (ELM). The hybrid architecture was used mainly to solve the classification task. [10] implemented the CNN and ELM architecture to classify Synthetic Aperture Radar (SAR) satellite's images from MSTAR database. The CNN was used to extract the features, while the ELM was used as the classifier. This research concludes that by using the hybrid architecture, the model is less prone to overfitting and, there was a speedup in reaching convergence, while still maintaining the high accuracy. [10] differed with our research as we tried to adopt the CNN and ELM hybrid architecture to classify the Buccal Mucosa comet assay rather than the SAR satellite's images.

[11] proposed the CNN-ELM method for hyperspectral images classification. The CNN-ELM hybrid method improved the accuracy over previous researches, reaching an accuracy score of 93.3% over Pavia University dataset, 98.85% on Pavia Center dataset, and 94.13% on AVIRIS Salinas dataset. [11] differed from our research by the dataset used, the CNN architecture, and the CNN training scheme as they conducted a one iteration CNN.

[12] proposed the CNN-ELM for age and gender classification. with enhancement in CNN feature extraction that resulted in 52.3% for age classification accuracy and 88.2% for gender classification accuracy on MORPH-II database. [12] also stated that the CNN-ELM hybrid method outperformed other researches in terms of accuracy and efficiency. [12] differed with our research as it used different CNN architecture and the dataset used was different.

In this research, we proposed a hybrid method of CNN and ELM to classify comet assay images, specifically the Buccal Mucosa. The CNN [13] was used to extract spatial features from the comet images, while the ELM [14] was used as a classifier. The use of ELM instead of multi-layered perceptron minimizes the risk of vanishing gradient,
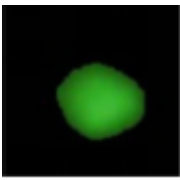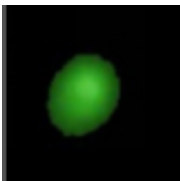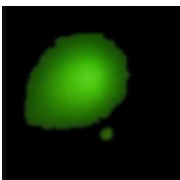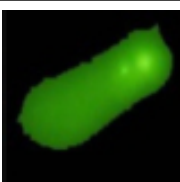
as it mainly consists of 1 input layer, 1 hidden layer, and 1 output layer. The simple architecture of ELM also causes the training time to be considerably short compared to other architecture. We also implemented data augmentation scheme in order to solve the problem of small amounts of data. The contribution of this paper is a novel way to assess the degree of damage from Buccal Mucosa comet assays using a hybrid method of CNN and ELM. Our proposed model can reach high accuracy (96.96%) even for small amounts of training data using augmentation strategy. Our proposed model outperforms previous research for the same dataset [7,8].

This research is based on and a developed version of the authors' thesis [15]. We organized this paper as follows: Chapter 2 contains information about the comet assay dataset, Chapter 3 explains the method used in this research, Chapter 4 shows the findings and discussion derived from the results of the conventional and the hybrid architecture proposed in this study, and Chapter 5 contains the conclusion and future work.

2. **Dataset.**

2.1. **Data acquisition.** In this research, we used a dataset that was used by a previous study [8]. The dataset contains 65 segmented and enhanced Buccal Mucosa comet assay images with a resolution of $100 \times 100 \times 3$, which are divided into 5 different classes. Class 1 represents a comet assay without its tail, whereas Class 5 represents a comet assay with

TABLE 1. Example of Buccal Mucosa comet assay image from each class

Class	Comet assay image
1	
2	
3	
4	
5	

the longest tail is. The longer the tail is, the more severe the DNA damage is. These 65 images were then divided as follows: 11 data of Class 1; 13 data of Class 2; 9 data of Class 3; 25 data of Class 4; and 25 data of Class 5. Table 1 shows the example of images that belong to each class.

2.2. **Data preprocessing.** We apply a few preprocessing techniques to the dataset, described as follows.

1) Gray-scaling

The gray-scaling technique aims to convert images with RGB channels into 1 gray channel images with an intensity between [0-256]. We did the gray-scaling technique as green was the only dominant colour from all three channels. This technique transforms the resolution of the data from $100 \times 100 \times 3$ into $100 \times 100 \times 1$, which would reduce the computational training time due to smaller resolution. Equation (1) is used to convert the RGB images into gray-scale image, where $R_{x,y}$ is the intensity of red pixel, $G_{x,y}$ is the intensity of green pixel, $B_{x,y}$ is the intensity of the blue pixel, x is the pixel position on the x-axis, and y is the pixel position on the y-axis.

$$f(x, y) = 0.299 * R_{x,y} + 0.587 * G_{x,y} + 0.114 * B_{x,y} \tag{1}$$

The weights are taken based on the provisions of BT.601 from the International Telecommunication Union-Radiocommunication sector [16].

2) Morphological Opening

We used the morphological opening to remove noises that are insignificant to the comet and its tail. This method also amplified the boundaries between the comet and its background. In this research, we used a kernel with a size of 5×5 for the opening.

3) Augmentation

We implemented the augmentation technique as we were dealing with a tiny dataset that is prone to overfitting problems. The following operations were used to augment a single image, namely: *Rotation* (between -25 to 25), *Vertical Flip*, *Horizontal Flip*, Zoom (with magnification between 0.9 to 1.3 times).

2.3. **Train-test split.** We split the preprocessed data with 2 different schemes, namely Non-Augmented and Split-Augmentation. The Non-Augmented scheme was applied to the data before it was augmented. The 65 images were split into train-validation data with the ratio of 80 : 20. Data splitting with a ratio of 80% for training data and 20% for validation data is a splitting scheme that is often used in machine learning. The goal is that an architecture which has been trained with 80% training data can have its performance measured with the remaining 20% that the architecture has never seen before. Table 2 shows the result of the Non-Augmented scheme. The Split-Augmentation scheme is a scheme where the 65 images were split into train-validation data with a ratio

TABLE 2. Non-Augmented data split

Class	Amount of data	Train-test split	
		Train data	Validation data
1	11	8	3
2	13	10	3
3	9	7	2
4	25	20	5
5	7	5	2
Total	65	50	15

TABLE 3. Split-Augmentation data split

| Class | Amount of data | Train-test split | | Validation data |
| | | Train data augmentation | | |
		Before	After	
1	11	8	80	3
2	13	10	100	3
3	9	7	70	2
4	25	20	200	5
5	7	5	50	2
Total	65	50	500	15

of 80 : 20, and later the augmentation technique was applied to the training data only (Table 3).

3. Hybrid CNN-ELM.

3.1. **CNN as a feature extractor.** In this research, CNN [13,17-19] was used to capture spatial-space relation from all comet assay images. The CNN architecture consists of 3-layer groups, with each group containing 2 convolutional layers, 1 max-pooling layer, and 1 dropout layer (Figure 1). The deeper the layer group is, the number of filters will increase, and the filter size will decrease. In the training stage, the fully-connected layer was used as the classifier of the model. However, the fully-connected layer would be replaced with the ELM once the CNN model converged. Equation (2) shows how the kernel vector of the convolution process is applied to the input vector.

$$(I * K)_{i,j} = \sum_{m=0}^{k_1-1} \sum_{n=0}^{k_2-1} \sum_{c=1}^{c} I_{i+m,j+n,c} \cdot K_{m,n,c} + b \tag{2}$$

I is the input vector, K is the kernel vector, and c is the number of channels from input vector I. The general architecture of CNN as a feature extractor (input shape, output shape, kernel size, number of filters) is shown in Table 4.
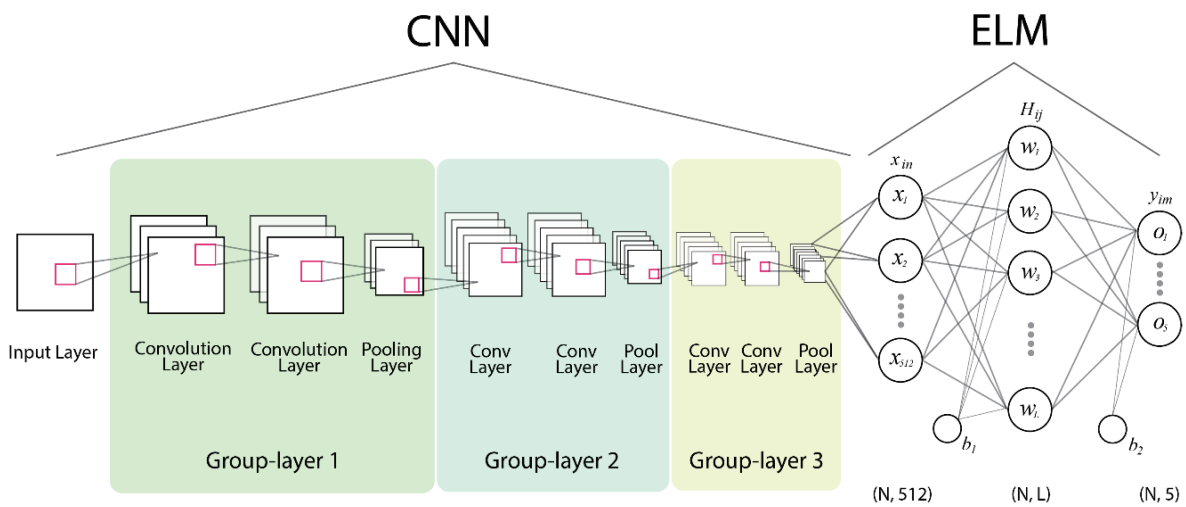

FIGURE 1. CNN-ELM architecture

TABLE 4. General architecture of the CNN

Layer	Input shape	Output shape	Description
Convolution 1	$(N, 100, 100, 1)$	$(N, 94, 94, 8)$	8 filters, 7×7 kernel
Convolution 2	$(N, 94, 94, 8)$	$(N, 90, 90, 8)$	8 filters, 7×7 kernel
Max-pooling 1	$(N, 90, 90, 8)$	$(N, 45, 45, 8)$	2×2 kernel
Convolution 3	$(N, 45, 45, 8)$	$(N, 39, 39, 16)$	16 filters, 7×7 kernel
Convolution 4	$(N, 39, 39, 16)$	$(N, 33, 33, 16)$	16 filters, 7×7 kernel
Max-pooling 2	$(N, 33, 33, 16)$	$(N, 16, 16, 16)$	2×2 kernel
Convolution 5	$(N, 16, 16, 16)$	$(N, 12, 12, 32)$	32 filters, 5×5 kernel
Convolution 6	$(N, 12, 12, 32)$	$(N, 8, 8, 32)$	32 filters, 5×5 kernel
Max-pooling 3	$(N, 8, 8, 32)$	$(N, 4, 4, 32)$	2×2 kernel
Flatten	$(N, 4, 4, 32)$	$(N, 512)$	
Dense	$(N, 512)$	$(N, 1024)$	ReLU, 1024 neurons
Output	$(N, 1024)$	$(N, 5)$	Softmax, 5 neurons

3.2. **ELM as a classifier.** ELM is a classifier which consists of 1 input layer, 1 hidden layer, and 1 output layer [14]. This simple architecture was proposed to minimize the effect of vanishing gradient that often occurs in the backpropagation process of deep fully-connected architecture. The ELM also offered faster training speed. The ELM used in this research received an input matrix with a resolution of $(N, 512)$ from the CNN and produced output with a resolution of $(N, 5)$ with N as the number of images (Figure 1). The following steps provide a brief illustration of the ELM architecture used in this research.

1) Initialize an input matrix $X_{i,n}$, which in this case, is the output from CNN, a matrix with a resolution of $(N, 512)$. $i = 1, 2, \ldots, N$ (N is number of data samples) and $n = 1, 2, \ldots, 512$ (512 is number of input layer neurons).

2) Determine input weights matrix, where $j = 1, 2, \ldots, L$ (L is the number of hidden neurons). The weights are initialized using either random normal or random uniform distribution, thus, resulting in input weights matrix with a resolution of $(512, L)$.

3) Determine output weights matrix $H_{i,j}$ (i is the i-th row of sample and j is the column of hidden neuron j). Each element in the matrix is the calculation result of the dot product between $x_{i,n}$ and $w_{n,j}$ added by b, and then processed by the activation function $g(w_j \cdot x_i + b_j)$. This step will result in a matrix with a size of (N, L). L will be determined by experiment parameters.

4) Determine output weights matrix β_{jm} using Equation (3), where H_{ij}^{τ} is pseudoinverse of Moore-Penrose matrix and t_{jm} is the vector target. The equation will result in an output weights matrix with a size of $(L, 5)$.

$$\beta_{jm} = H_{ij}^{\tau} \cdot t_{jm} \tag{3}$$

5) Determine the output y_{im} using Equation (4). The equation will result in output matrix y with row length of N and column length of m. The equation will result in a matrix with a resolution of $(N, 5)$.

$$y_{im} = H_{ij} \cdot \beta_{jm} \tag{4}$$

3.3. **Training stage.** The training stage is divided into 4 steps, namely, CNN kernel training, intermediate layer feature extraction, determining the weight of ELM, and predicting using the CNN-ELM hybrid. These steps were applied to the Non-Augmented and Split-Augmentation schemes. Firstly, the CNN kernels shown by Table 4 need to be trained to be able to capture spatial relations from each comet assay image. In this step,

batch training was used with each batch containing 20 images. When the CNN converged, the training stops and the fully-connected layer would be replaced by an ELM classifier. For the next step, we modified the CNN model by removing the fully-connected layer. This step caused the model to produce a feature matrix with a resolution of $(N, 4, 4, 32)$ which is then flattened into a matrix with a resolution of $(N, 512)$. Afterwards, the weights of the ELM need to be initialized. The input weights were randomly generated with either normal random or uniform random distribution. The output weights were obtained from the dot product between Moore-Penrose pseudoinverse of the matrix with target matrix as shown in Equation (4). The feature data extracted from the modified CNN model was then predicted using the ELM defined in the previous step. Figure 2 showed the detailed training stage of the CNN-ELM architecture. To measure the quality of our models, we used an accuracy metric which can be calculated using Equation (5).

$$\text{Accuracy} = \frac{\text{TP} + \text{TN}}{\text{TP} + \text{TN} + \text{FP} + \text{FN}} \tag{5}$$
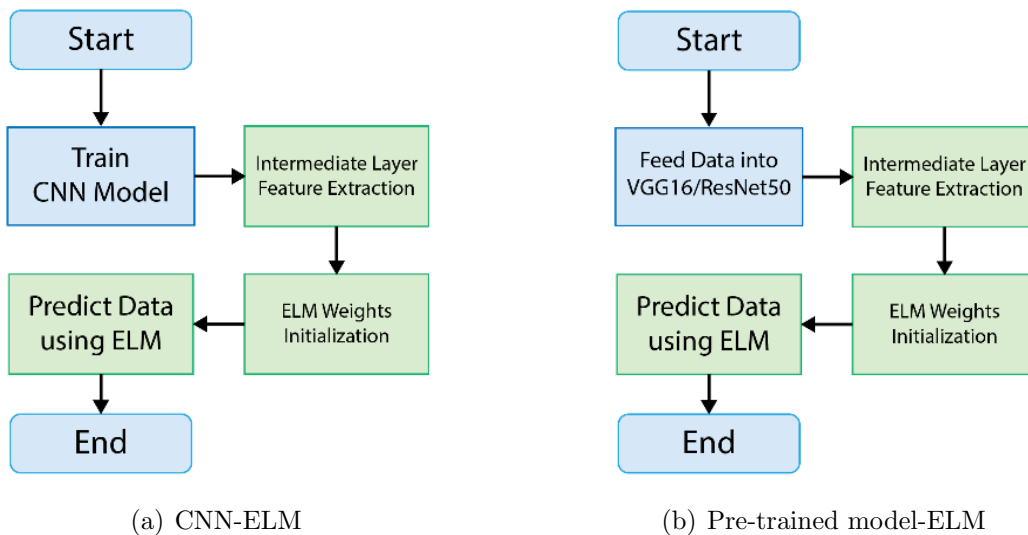

(a) CNN-ELM   (b) Pre-trained model-ELM

FIGURE 2. Training stage flowchart

3.4. **VGG16 and ResNet50 as a feature extractor.** VGG16 [20] and ResNet50 [21] are two pre-trained models that have millions of parameters trained with ImageNet data. These models are often used in the image classification task, as they can store knowledge obtained from prior training and applying it to another problem [8]. In this research, we tried to utilize transfer learning from both models and combine them with the ELM classifier (Figure 2). The VGG16 and ResNet50 were used as a feature extractor, while ELM was used as a replacement for the fully-connected layer of both models. We compared our hybrid CNN-ELM model with VGG16-ELM and ResNet50-ELM. This comparison was intended to know the performance of our architecture compared to other popular architecture. Similar training stages were applied into both VGG16 and ResNet50, with the two only differences which were the kernel training step is skipped and the data resolution produced by the intermediate layer feature extraction step was $(N, 4608)$ for VGG16 and $(N, 32768)$ for ResNet50.

4. Results and Discussion.

4.1. Hybrid CNN-ELM. We trained the hybrid CNN-ELM architecture using each data split scheme (Table 5), where we also observed the impact of the number of epochs towards the accuracy score and training time (Table 6). From the result (Table 5), it seems that the Split-Augmentation scheme took the longest training time compared to other schemes due to the larger amount of data. However, the Split-Augmentation scheme scored the highest accuracy rates, followed by the Non-Augmented scheme. The score for the Non-Augmented scheme was quite low, maxed at 44.66%. On the other hand, the scheme that implemented Augmentation technique scored a far better score, reaching 96.96% for Split-Augmentation scheme. It is quite self-explanatory that the Non-Augmented scheme did not perform well because of its small dataset size. Aside from that, the number of epochs increased along with the accuracy score for Non-Augmented, but the opposite happened to the Split-Augmentation.

TABLE 5. Accuracy and training time by split scheme and epochs

Split scheme	Epochs	Accuracy	Training time (s)
Non-Augmented	10	38.66%	34.44
	20	39.33%	65.9
	30	44.66%	99.69
Split-Augmentation	**10**	**96.96%**	**193.49**
	20	93.97%	848.19
	30	91.46%	2093.92

TABLE 6. Accuracy and training time by random weights type and number of neurons

Random types	Number of neurons	Accuracy	Training time (s)
Uniform	1024	65.4%	285.71
	2048	63.52%	495.03
	4096	71%	1427.93
Normal	**1024**	**95.09%**	**276.2**
	2048	93.89%	400.61
	4096	93.21%	1383.09

We also observed the impact of random weight initialization technique for the ELM (Table 6). In this experiment, we utilized the Split-Augmentation scheme as it produced a higher accuracy score compared to other scheme. The model that used random uniform scored lower than the model that utilized random normal for its weight initializer. The uniform weighted model scored an accuracy maxed at 71%, while the normal weighted model scored 95.09% for its highest. However, the increasing number of neurons did prolong the training time but did not show a pattern of increasing accuracy scores. Thus, we believe that random normal weights initialization for the CNN-ELM hybrid method is the better choice compared to the random uniform.

4.2. Hybrid VGG16-ELM and hybrid ResNet50-ELM. Aside from CNN-ELM hybrid architecture, we also implemented two additional architectures, namely the VGG16-ELM and ResNet50-ELM. We observed the relation between each pre-trained model and the dataset split scheme (Table 7). Both pre-trained models failed to score high accuracy

TABLE 7. Accuracy and training time by split scheme and pre-trained model

Split scheme	Pre-trained model	Accuracy	Training time (s)
Non-Augmented	VGG16	50.66%	5.85
	ResNet50	25.33%	5.23
Split-Augmentation	**VGG16**	**88.4%**	**40.99**
	ResNet50	76.8%	23.16

TABLE 8. Accuracy and training time by random weights type and number of neurons

Class	Comet assay image	Accuracy	Training time (s)
Uniform	1024	90.99%	40.26
	2048	**91.4%**	**46.39**
	4096	90.5%	105.18
Normal	1024	88.8%	40.5
	2048	**91.19%**	**48.47**
	4096	90.48%	105.3

using the Non-Augmented scheme, as the dataset is considered as a tiny dataset and training with tiny dataset often results in a bad accuracy score. The VGG16-ELM reached the highest accuracy while using the Split-Augmentation scheme, scoring about 88.4%, followed by the ResNet50-ELM (76.8%) using the same Split-Augmentation scheme. From Table 7, it can be concluded that VGG16-ELM outperformed ResNet50-ELM in terms of accuracy, although it took a slightly longer training time.

We then fine-tuned the ELM for the best pre-trained hybrid method, VGG16-ELM architecture. We conducted a random weights initialization and number of neurons experiment, with the result tabulated in Table 8. The accuracy scores of the random weights experiments were not far apart and the number of neurons did not seem to affect the accuracy score. However, the random uniform with 2048 neurons did score the highest accuracy (91.4%) compared to other combinations of random weights and number of neurons.

4.3. **Comparison of hybrid methods.** The CNN-ELM hybrid method scored a higher accuracy score compared to VGG16-ELM and ResNet50-ELM (Table 9), scoring 8.56% higher than the VGG16-ELM and 20.16% higher than the ResNet50-ELM architecture. We believe this happened because the pre-trained hybrid methods were trained for a more general task rather than specifically for comet assay classification tasks, while our CNN-ELM was the opposite. However, in terms of training time, the pre-trained-ELM hybrid consumed far lower time compared to the CNN-ELM architecture but still maintained reasonably good accuracy scores. This happened because we did not train the pre-trained VGG16 and ResNet50.

TABLE 9. Accuracy comparison with previous research

Model	Accuracy
CNN-ELM	96.96%
VGG16-ELM	88.4%
ResNet50-ELM	76.8%
VGG16-MLP [8]	70.5%
OpenComet [7]	11.5%

4.4. **Comparison with previous works.** Comparison of the performance of our model is very limited because previously there were only a few researches on the Buccal Mucosa comet assay classification. We compared our models with two models from previous researches [7,8]. Our work was closely related to the VGG16-MLP architecture [8] but performed better even when the only differences are the classifier and the augmentation technique. [8] used 1 hidden layer multi-layered perceptron with 300 neurons as its classifier. We suspected that ELM performs better than the MLP as MLP generally performs well when used in a deep architecture. However, as the MLP went deeper, it is becoming more prone to vanishing gradient problems. Thus, we believe that by using ELM instead of MLP, we minimize the risk of the vanishing gradient and simultaneously maintaining the good accuracy score. [8] also implemented different augmentation techniques, where their augmented data had a size of 250 and our data had at least 500 images for training data. This also can be the cause of why our proposed hybrid architecture performs better on classifying comet assay compared to their model. Our model also performed better compared to OpenComet tools [7], where the OpenComet only managed to achieve an accuracy of 11.5% when using the same dataset. We suspect that the very low score on the OpenComet tool is because it was designed for samples from cultured lymphocyte cells which have very low noise, in contrast to the data we used where Buccal Mucosa has high noise because it was taken using the swab technique. However, we were unable to compare the computation time with previous researches [7,8] due to the absence of computation time in these researches.

5. **Conclusion.** We have proposed and shown how to detect damaged DNA using comet assay images and hybrid CNN-ELM architecture. We used CNN to extract spatial relation features from the comet assay images and use the ELM as a substitute for CNN's classifier. The ELM was proposed to replace the fully-connected layer as a fully-connected layer uses backpropagation technique which is prone to vanishing gradient problems and is often time-consuming. By using ELM, we also minimize the risk of vanishing gradient problems and fasten the prediction time. We trained on the dataset using 2 different schemes, namely Non-Augmented and Split-Augmentation. The augmentation step was intended to increase the dataset size, thus resulting in a model with a good classification capability. Our hybrid CNN-ELM model obtained 96.96% for accuracy score, followed by the hybrid VGG16-ELM and ResNet50-ELM (88.4% and 76.8% respectively). There is still a shortcoming in this research, namely the segmentation process of Buccal Mucosa comet assay is still done manually. This deficiency will have a big impact when more and more data is used. Therefore, we recommend applying an automatic segmentation process so that it can handle large amounts of data.

REFERENCES

[1] A. R. Collins, The comet assay for DNA damage and repair: Principles, applications, and limitations, *Mol. Biotechnol.*, vol.26, no.3, pp.249-261, 2004.
[2] R. D. Yanuaryska, Comet assay assessment of DNA damage in Buccal Mucosa cells exposed to X-rays via panoramic radiography, *Journal of Dentistry Indonesia*, vol.25, no.1, pp.53-57, 2018.
[3] J. F. Muniz, L. A. McCauley, V. Pak, M. R. Lasarev and G. E. Kisby, Effects of sample collection and storage conditions on DNA damage in buccal cells from agricultural workers, *Mutation Research/Genetic Toxicology and Environmental Mutagenesis*, vol.720, pp.8-13, 2011.

[4] N. K. Mondal, P. Bhattacharya and M. R. Ray, Assessment of DNA damage by comet assay and fast halo assay in buccal epithelial cells of Indian women chronically exposed to biomass smoke, *International Journal of Hygiene and Environmental Health*, vol.214, no.4, pp.311-318, 2011.

[5] K. Konca, A. Lankoff, A. Banasik, H. Lisowska, T. Kuszewski, S. Gozdz, Z. Koza and A. Wojcik, A cross-platform public domain PC image-analysis program for the comet assay, *Mutation Research/Genetic Toxicology and Environmental Mutagenesis*, vol.534, pp.15-20, 2003.

[6] Y. Lu, Y. Liu and C. Yang, Evaluating *in vitro* DNA damage using comet assay, *Journal of Visualized Experiments*, vol.128, DOI: 10.3791/56450, 2017.

[7] B. M. Gyori, G. Venkatachalam, P. S. Thiagarajan, D. Hsu and M. Clement, OpenComet: An automated tool for comet assay image analysis, *Redox Biology*, vol.2, pp.457-465, 2014.

[8] E. Anarossi, Afiahayati, R. D. Yanuaryska, F. U. Nuha and S. Mulyana, Comet assay classification for Buccal Mucosa's DNA damage measurement with super tiny dataset using transfer learning, *Intelligent Information and Database Systems: Recent Developments*, vol.830, pp.279-289, 2019.

[9] O. P. Barus and N. Surantha, The classification of arrhythmia using the method of extreme learning machine, *ICIC Express Letters*, vol.14, no.12, pp.1147-1154, 2020.

[10] P. Wang, X. Zhang and Y. Hao, A method combining CNN and ELM for feature extraction and classification of SAR image, *Journal of Sensors*, 2019.

[11] F. Cao, Z. Yang, J. Ren and B. W. Ling, Convolutional neural network extreme learning machine for effective classification of hyperspectral images, *Journal of Applied Remote Sensing*, vol.12, no.3, 2018.

[12] M. Duan, K. Li, C. Yang and K. Li, A hybrid deep learning CNN-ELM for age and gender classification, *Neurocomputing*, vol.275, pp.448-461, 2018.

[13] I. Goodfellow, Y. Bengio and A. Courville, *Deep Learning*, MIT Press, https://www.deeplearning book.org/, 2016.

[14] G.-B. Huang, Q.-Y. Zhu and C.-K. Siew, Extreme learning machine: A new learning scheme of feedforward neural networks, *2004 IEEE International Joint Conference on Neural Networks (IEEE Cat. No. 04CH37541)*, vol.2, pp.985-990, 2004.

[15] Y. Tadrik, *CNN-Extreme Learning Machine Method for DNA Damage Classification Using Comet Assay (Metode CNN-Extreme Learning Machine Untuk Klasifikasi Kerusakan DNA Menggunakan Comet Assay)*, Bachelor's Thesis, Department of Computer Science and Electronics, Universitas Gadjah Mada, Yogyakarta, Indonesia, 2020.

[16] RECOMMENDATION ITU-R BT, *Studio Encoding Parameters of Digital Television for Standard 4 : 3 and Wide-Screen 16 : 9 Aspect Ratios*, International Telecommunications Union, 2011.

[17] R. A. Rajagede, C. K. Dewa and Afiahayati, Recognizing arabic letter utterance using convolutional neural network, *2017 the 18th IEEE/ACIS International Conference on Software Engineering, Artificial Intelligence, Networking and Parallel/Distributed Computing (SNPD)*, pp.181-186, 2017.

[18] J. Kurniawan, S. G. S. Syahra, C. K. Dewa and Afiahayati, Traffic congestion detection: Learning from CCTV monitoring images using convolutional neural network, *Procedia Computer Science*, vol.144, pp.291-297, 2018.

[19] M. Dwiastuti and Afiahayati, Speech recognition for people with dysarthria using convolutional neural network, *ICIC Express Letters, Part B: Applications*, vol.10, no.9, pp.849-858, 2019.

[20] K. Simonyan and A. Zisserman, Very deep convolutional networks for large-scale image recognition, *arXiv.org*, arXiv: 1409.1556, 2014.

[21] K. He, X. Zhang, S. Ren and J. Sun, Deep residual learning for image recognition, *Proc. of the IEEE Conference on Computer Vision and Pattern Recognition*, pp.770-778, 2016.